Constance Rost-Bietsch (Autor)

Ambipolar and Light-Emitting Organic Field-Effect Transistors

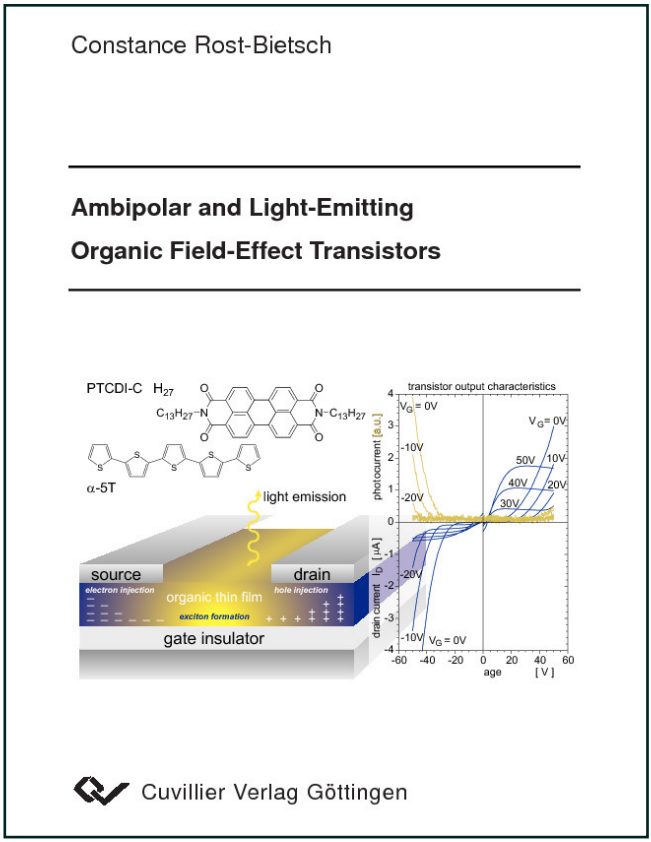

https://cuvillier.de/de/shop/publications/2507

Chapter 1

Introduction

1.1 State of the Art of OFETs

The principle of the field-effect transistor (FET) was introduced by Lilienfield in 1930 [Lil30] and applied to organic semiconductors for the first time in 1970 for phthalocyanine single crystals [Bar70] as well as for the organic semiconductor chloranil [Pet70], followed by field-effect measurements of organic dye films in 1984 [Kud84]. In the late 80's, several researchers began investigating small-molecule organic materials with highly delocalized π-electron systems. The strategy to increase intermolecular transport was to improve the π-orbital overlap of adjacent molecules in highly oriented thin films of these materials.

Since then, organic materials have been successfully incorporated as active layers in electronic thin-film devices, such as organic light-emitting diodes (OLEDs) [Tan87, Bur90, Bei02, Rie03], organic solar cells [Peu03, Sha01], and organic field-effect transistors (OFETs) [Ebi83, Kud84, Hor89, Tsu86, Koe87, Sir98]. The devices are based on either conjugated polymers [Bur90, Sha01, Ebi83, Tsu86, Koe87, Sir98] or small molecules [Tan87, Peu03, Kud84, Hor89, Bei02, Rie03]. For example, OLEDs find broad application in display devices [Raj00, Ter03]. The progress was recently highlighted by the demonstration of a 20-inch full-color active-matrix OLED display driven by a-Si thin-film transistors [Tsu03, Rie04]. OFETs are being developed as switching devices for active-matrix OLED displays [Jac98] and for low-cost electronics, such as low-end smart cards and electronic identification tags [Gmb04]. The growing interest in organic-based thin-film electronics is not only due to its immense progress in performance, but also due to the potential flexibility of the devices, their relatively easy processing and low production costs. Organic thin films can be deposited and processed by thermal evaporation, spin-coating, micro-contact printing, self-assembly or screen-printing.

Typically, in organic materials unipolar transport is observed, i.e. one type of charge carrier is transported preferentially, therefore a transistor operates either as *p*- or *n*-

channel device. In Figure 1.1 the molecular structures of materials used for charge-transport layers in OFETs are shown. The prime example for materials used in *p*-type OFETs is pentacene: For evaporated thin films, mobilities of up to 2.2 cm^2/Vs have been reported [Lin97] with a corresponding on/off current ratio of more than 10^8. For devices with such a high mobility, nearly temperature-independent transport has been reported [Nel98], indicating that a simple transport model of thermally activated hopping cannot be applied. These values can easily compete with those of devices fabricated from amorphous silicon, which have a charge-carrier mobility of about 1 cm^2/Vs [Tsu03] and are limited to on/off current ratios of 10^6. However, it has to be noted that OFETs are typically driven at much higher voltages, i.e. up to ± 100 V, than amorphous silicon thin-film transistors (TFTs). Another group of well-studied hole-transport materials are oligothiophenes (see Fig. 1.1): the first α-6T [1] based OFET was reported already in 1989 [Hor89]. The extracted hole mobility increased due to improvements in film preparation from initially 2.2×10^{-2} cm^2/Vs [Gar89] to 1×10^{-1} cm^2/Vs [Hal03]. Oligophenyl, another class of small molecules with a relatively high hole mobility, were introduced for OFETs in 1997 [Gun97]. Here, the mobility increases with the chain length, that is from *p*-4P [2], *p*-5P [3] to *p*-6P [4] from 1×10^{-2} cm^2/Vs, 4×10^{-2} cm^2/Vs to 7×10^{-2} cm^2/Vs, respectively, and on/off current ratios of 10^5 to 10^6 have been reported. The increase in mobility with increasing chain length was also observed for the other systems discussed above and was explained by an increased molecular order within the thin film. A detailed study of the relation between molecular order and charge-carrier mobility can be found in [Mue01]. Furthermore, *p*-channel devices have been fabricated from nickel phthalocyanine [Gui89] and copper-phthalocyanine [Bao96] with hole mobilities of 7×10^{-4} cm^2/Vs and 2×10^{-2} cm^2/Vs, respectively. The highest hole mobility in organic materials reported so far is up to 20 cm^2/Vs for rubrene single crystals [Pod03, Pod04, Sta04].

The choice of electron-transport materials is rather limited and in general, the charge-carrier mobilities are lower. *n*-channel devices have been fabricated using C_{60}, naphthalene and perylene derivatives, fluorinated copper-phthalocyanine and fluorinated oligothiophene derivatives. For the perylene derivative PTCDI-C_8H_{17} [5] an electron mobility of 0.6 cm^2/Vs with a corresponding on/off current ratio $> 10^5$ was reported [Mal02]. The first *n*-type sexithiophene was published in 2000 [Fac00], and electron mobilities of 10^{-3} cm^2/Vs and 4.8×10^{-2} cm^2/Vs were reported for DFH-6T [6] and DFH-4T [7], respec-

[1] α-sexithiophene
[2] *para*-quaterphenyl
[3] *para*-quinquephenyl
[4] *para*-sexiphenyl
[5] N,N'-dioctyl-3,4,9,10-perylene tetracarboxylic diimide
[6] α,ω-diperfluorohexylsexithiophene
[7] α,ω-diperfluorohexylquaterthiophene

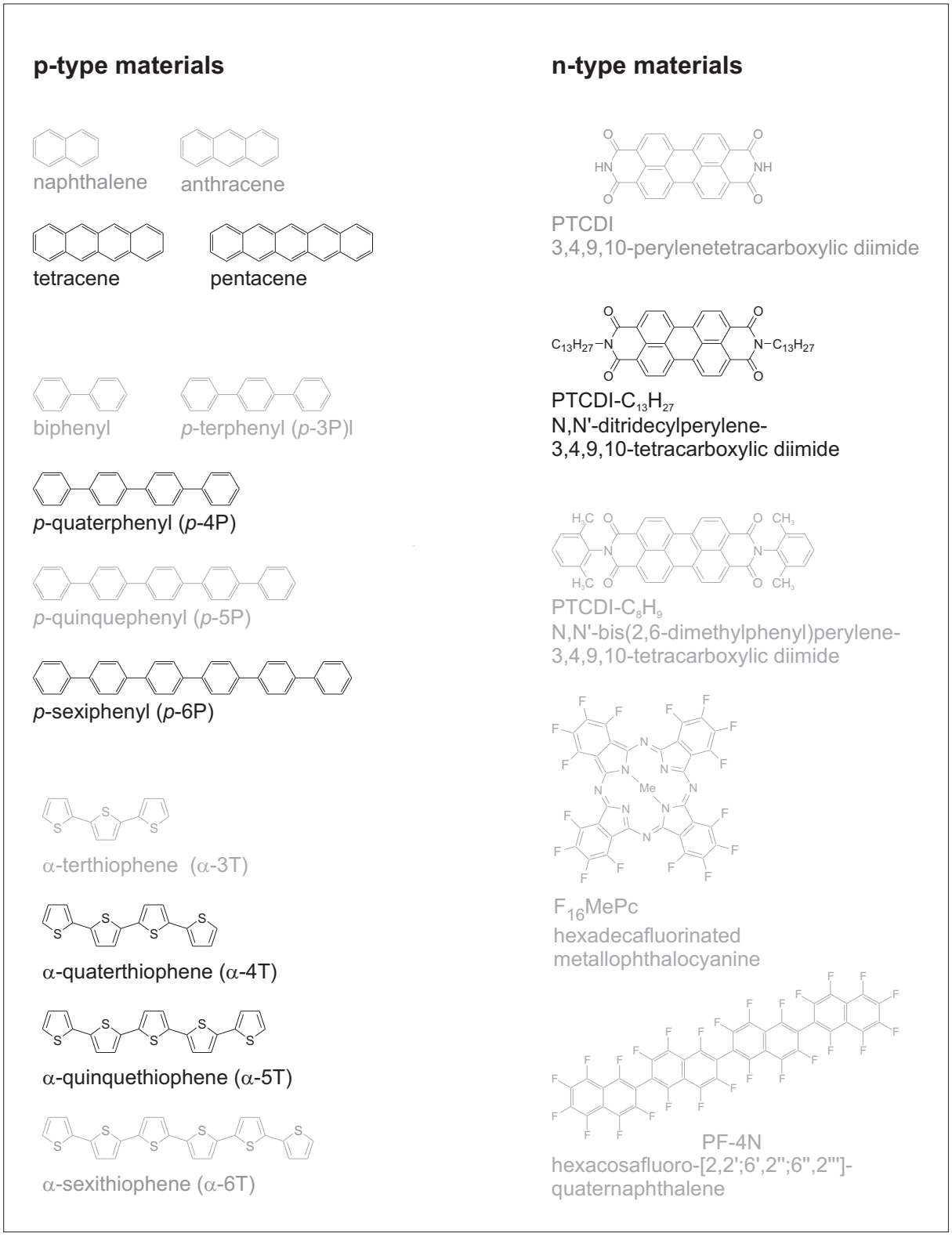

Figure 1.1: *Molecular structures of materials used for charge-transport layers in OFETs. The compounds investigated in this work are shown in black.*

tively [Fac03]. Moreover, fluorinated copper-phthalocyanine *n*-channel transistors [Bao98] have been combined with *p*-channel devices in integrated circuits [Cro01]. Perfluorinated *n*-type oligophenylenes [Hei00] have not yet been successfully employed in OFETs so far.

Extensive reviews on unipolar organic field-effect devices can be found in Refs. [Hor90, Kat97, Hor98, Dim01, Dim02]. Further improvement of single-layer OFETs will depend on the design and synthesis of new transport materials, improvements in device geometry, as well as optimization of device fabrication. The main disadvantage of OFETs as compared with conventional amorphous Si TFTs does not originate in its intrinsic material properties, but in the high contact resistance that requires relatively large device dimensions, i.e. in the micrometer range, leading to high operation voltages. In the case of shorter channel dimension, the device characteristics are dominated by the contact resistance instead of the channel properties.

In contrast to inorganic materials, where ambipolar device characteristic is well understood and described in detail, e.g. for amorphous silicon FETs [Pfl86a, Pfl86b, Neu87a], in organic devices typically unipolar transport is observed. Because pure organic semiconductors are intrinsic and exhibit no significant difference between the electron and the hole mobility, the unipolar transport characteristic observed in organic semiconductors has been attributed to impurities [Kar03]. Ambipolar transport in a single organic material [8] has so far been reported only for titanyl-phthalocyanine [Tad00], DCMT [9] [Che03b] and pentacene [Mei03] thin films as well as for carbon nanotubes (CNTs) [Mar01, Lin04a, Shi04]. The ambipolarity of CNTs has been proposed for application in nonvolatile molecular memory elements [Rad02]. In case of titanyl-phthalocyanine, ambipolar transport was observed in a transition state between unipolar electron and hole transport, initiated by oxygen exposure. The unipolar electron mobility was 9×10^{-6} cm^2/Vs, and the unipolar hole mobility 1×10^{-5} cm^2/Vs. The ambipolar electron and hole mobilities were even lower, with 2.7×10^{-6} cm^2/Vs and 2×10^{-6} cm^2/Vs, respectively. Thus, the ambipolarity in titanyl-phthalocyanine has no potential application in integrated circuits. Also for DCMT, the ambipolar mobilities, with $< 10^{-4}$ cm^2/Vs, were much lower than in the unipolar *n*-channel device, for which an electron mobility of 0.2 cm^2/Vs has been reported. In the case of pentacene the reported electron mobility of 10^{-6} cm^2/Vs could be observed only in vacuum; its hole mobility is 10^{-2} cm^2/Vs [Mei03]. This result is consistent with the observation of electron accumulation below the contact in in-situ characterized pentacene thin films described in Chapter 4 of this thesis.

[8] Previously reported results on ambipolarity and light emission combined with observed lasing in organic single crystals had to be withdrawn due to scientific misconduct. For details see also *Report on the investigation committee on the possibility of scientific misconduct in the work of Hendrik Schön and coauthors*, September 2002. http : //www.lucent.com/news_events/pdf/researchreview.pdf

[9] 3'4'-dibutyl-5,5"bis(dicyanomethylene)-5,5"dihydro-2,2':5',2"-terthiophene

Another approach for the fabrication of ambipolar OFETs was therefore the combination of an electron- and a hole-transport material in a bilayer heterostructure, as it has been shown for the combination of C_{60} and α-6T as well as PTCDA [10] and H6T [11] [Dod95, Dod96]. A drawback of this structure is the limitation to symmetrical source and drain contacts, leading to a large injection barrier for at least one type of charge carrier. A pronounced ambipolar characteristic for a bilayer heterostructure OFET consisting of pentacene and PTCDI-$C_{13}H_{27}$ [12], which uses different contact metals for the source and the drain electrode to achieve efficient electron and hole injection [Ros04a], is discussed in detail in Chapter 5 of this thesis. This work has triggered further research on the influence of injection barriers and the contact resistance on the ambipolar characteristic of bilayer heterostructure OFETs [Kuw04].

For future technological application it would probably be advantageous to combine both materials in a single layer. An ambipolar transistor based on a blend of a *p*-type polymer, MDMO-PPV [13], and a soluble derivative of C_{60}, PCBM [14], i.e. a blend of two otherwise unipolar materials, was reported for the first time in 2000 [Gee00]. The composition of blend films has an influence on the electron and hole mobility, as shown in [Pac03] for the combination of polyfluorene and PCBM. The ambipolar characteristic of a film consisting of the *n*-type-polymer BBL [15] and the *p*-type small-molecule copper-phthalocyanine was improved by increasing the crystallinity of the copper-phthalocyanine phase [Bab04]. Very recently, CMOS inverter circuits were fabricated using a blend of PCBM and OC_1C_{10}-PPV [16] [Mei03].

Ambipolar transport in a mixture of small molecules has been shown for single crystals of the quasi-one-dimensional Mott-Hubbard insulator (BEDT-TTF)[17](F_2TCNQ)[18] [Has04]. The hole mobility in these crystals is $\sim$1.5 times larger than the electron mobility and shows at a temperature of $T = 40$ K a value of $\mu = 2 \times 10^{-3}$ cm^2/Vs. For coevaporated thin films ambipolar transport was reported for the first time for α-5T [19] and PTCDI-$C_{13}H_{27}$ [Ros04b]. The striking feature, however, was the simultaneous observation of electroluminescence (EL), which could be tuned by the applied gate bias. This concept will be discussed in detail in Chapter 6 of this thesis.

[10] perylene-3,4,9,10-tetracarboxylic-3,4,9,10-dianhydride
[11] α,ω-dihexylsexithiophene
[12] N,N'-ditridecylperylene-3,4,9,10-tetracarboxylic diimide
[13] poly(2-methoxy-5-(3,7-dimethyloctyloxy)-1,4-phenylenevinylene
[14] (6,6)-phenyl C61-butyric acid methyl ester
[15] poly(benzobisimidazobenzophenanthroline)
[16] poly[2-methoxy-5-(3',7'-dimethyloctyloxy)]-*p*-phenylene vinylene
[17] bis(ethylenedithio)tetrathiafulvalene
[18] 2.5-difluorotetracyanoquinodimethane
[19] α-quinquethiophene

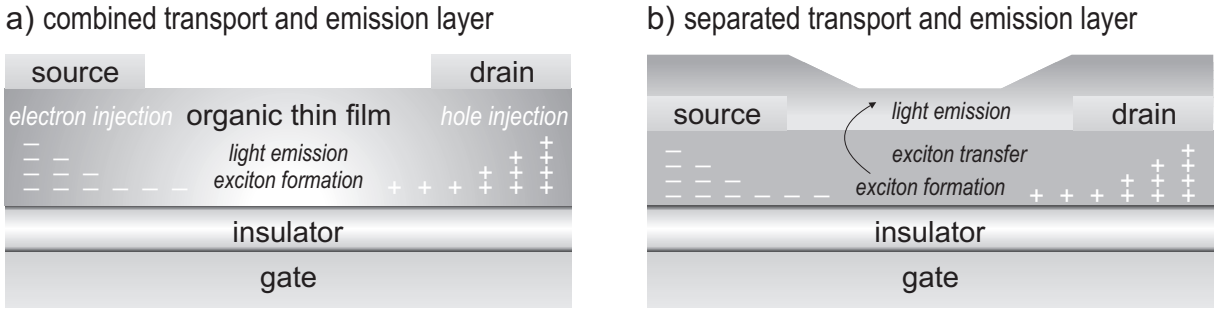

Figure 1.2: *Device structures of light-emitting field-effect transistors. (a) Within a one-layer structure, charge-carrier transport and light emission occurs in the same film. (b) In a two-layer structure, charge-carrier transport and exciton formation are spatially separated from light emission. This requires efficient energy transfer between the two layers. It should be noted that the device dimensions are not shown in scale: the active device thickness is typically in the order of 100 nm and the source-drain contact distance, i.e. the channel length L is typically in the order of 100 μm).*

1.2 Concept of Light Emission from OFETs

Combining light emission with switching characteristics in a single device, i.e. a light-emitting field-effect transistor, is interesting from both a scientific aspect as well as a technical point of view. On one hand it can give further insight into the understanding of fundamental device physics, on the other hand it would increase the number of potential applications of organic opto-electronic devices. Similarly to light emission in an OLED, light emission from an OFET requires electron and hole injection and transport as well as exciton formation followed by efficient radiative decay. Thus, ambipolar charge-carrier injection and transport are thought to be required for an efficient light-emitting OFET. Recently, in unipolar *p*-type tetracene thin-film OFETs [Hep03, San04] as well as in unipolar polymer OFETs [Ahl04, Sak04] EL was reported. However, the recombination zone and therefore also the EL in these unipolar OFETs is restricted to a region in close vicinity of the drain contact [Hep03, Rey04], resulting in quenching by the metal drain contact. In ambipolar devices, the recombination zone can be shifted between source and drain contact by the gate voltage, as it has been reported for ambipolar carbon nanotube FETs [Fre04].

The emitting material can either function as both emitting and transport material, or it can be placed on top of the transport layer and EL is based on exciton transfer. Figure 1.2 shows the two different concepts of light emission from a FET. From an electrical point of view both devices function identically: Electrons and holes are injected at source and drain contacts and the accumulation of both types of charge-carriers in a conductive channel is controlled by the gate electrode. In Figure 1.2(a), charge-carrier

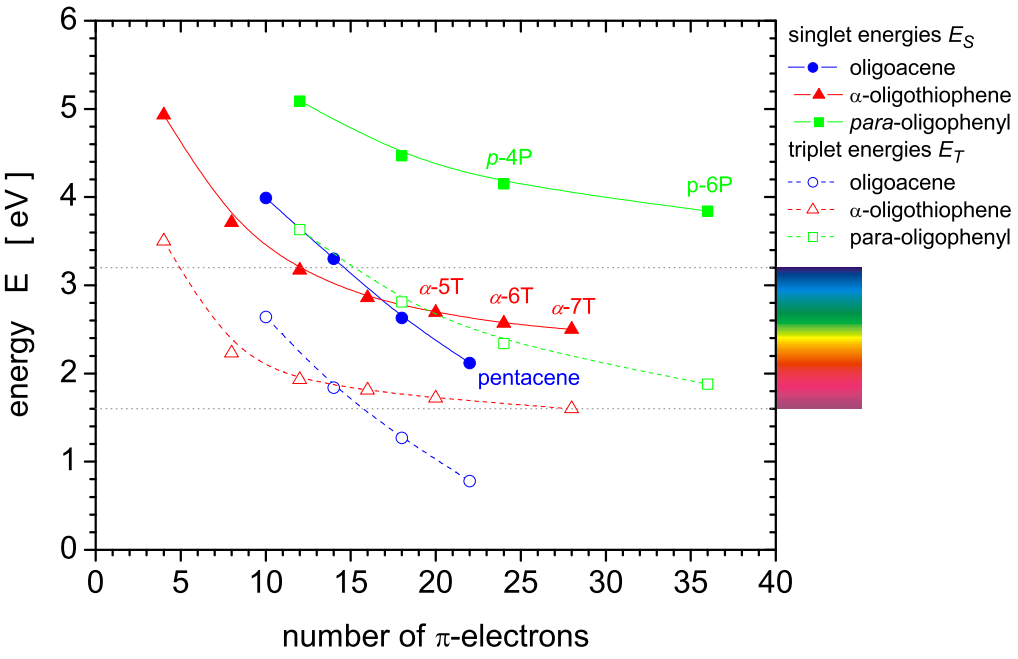

Figure 1.3: *Singlet (filled symbols) and triplet (hollow symbols) energies of materials for charge-transport layers in a light-emitting field-effect transistor. The values are taken from Table 1.1. The groups of materials considered are oligoacenes, α-oligothiophenes and para-oligophenyls. In addition, the spectral range of visible light is indicated.*

transport and light emission is allocated to a single layer. Thus, the EL is quenched by free charge carriers. In Figure 1.2(b), the charge-carrier transport is spatially separated from light emission occurring in a second layer on top of the transport layer. Thus, quenching by free charge-carriers is prevented, however, the EL is decreased by transfer losses. The transfer rate depends on the intermolecular distance of donor and acceptor and can be improved by decreasing the thickness of the transport layer, which however as a consequence impairs the transport properties. Typical transfer radii for Förster and Dexter transfer are a 5−10 nm or 1.5−2 nm, respectively. If the emission layer comprises a sufficient concentration of a phosphorescent dye, the diffusion length of triplet excitons will also contribute to the EL. The concept of separating the transport and the emission layer is one of the subject of a European Project (ILO[20]).

Figure 1.3 shows the singlet and triplet energies for typical hole-transport materials, which are also listed in Table 1.1. In addition, the spectral range of the visible spectrum is presented. In general, the energy gap of the transport material has to be larger than or within the visible spectrum. From an energetic point of view, materials from the class of *para*-oligophenyls are the most promising ones. However, their transport properties

[20]**I**njection **L**asing in **O**rganic Thin Films; contract number IST-2001-33057

Material	E_S [eV]	ϕ_{fl}	E_T [eV]	ϕ_T	Ref.	LUMO [eV]	HOMO [eV]	E_g [eV]	Ref.
naphthalene	3.99	0.19	2.62	0.75	[Mur93]	1.2-1.4	6.5-6.7	5.1-5.5	[Kar01a]
anthracene	3.30	0.30	1.84	0.71	[Mur93]	2.0-2.2	5.8-5.9	3.6-3.9	[Kar01a]
tetracene	2.63	0.17	1.27	0.62	[Mur93]	2.2-2.3	5.2-5.4	2.9-3.2	[Kar01a]
pentacene	2.12	0.08	0.78	0.16	[Mur93]	2.6-2.8 3.22	5.0-5.2 5.07	2.2-2.6 1.85	[Kar01a] [Sch02a]
thiophene	4.93	–	3.50	–	[dM99]				
α-2T	3.71	–	2.23	0.94	[dM99]				
α-3T	3.17	–	1.93	0.93	[dM99]				
α-4T	2.86	–	1.81	0.71	[dM99]				
α-5T	2.69	–	1.72	0.60	[dM99]		5.3		[Jon90]
α-6T	2.57	–	1.73	–	[Pog02]				
α-7T	2.50	–	1.60	0.60	[dM99]				
biphenyl	5.09	–	3.63	–	[Pog02]				
p-3P	4.47	–	2.81	–	[Pog02]				
p-4P	4.15	–	2.34	–	[Pog02]				
p-6P	3.84	–	1.88	–	[Pog02]	2.27	6.07	3.8	[Sch02b]
perylene	2.85	0.75	1.53	0.014	[Mur93]				
PTCDI-CH_3						3.4	5.4	2.0	[Hir95]

Table 1.1: *Singlet (E_S) and triplet (E_T) energies, fluorescence quantum yield (ϕ_{fl}), triplet quantum yield (ϕ_T), HOMO and LUMO levels of materials to be used as charge-transport layer in a light-emitting field-effect transistor. The groups of materials considered are oligoacenes, α-oligothiophenes and para-oligophenyls, all of which are p-type materials, and PTCDI-CH_3 with a similar molecular structure as PTCDI-$C_{13}H_{27}$ as n-type material. Values cited from [Mur93] and [dM99] were derived in solution from optical absorption measurements. Thus, these values depict only an indication for the actual HOMO-LUMO separation E_g, since they do not account for exciton binding energies. The same counts for the value of E_g in case of p-6P [Sch02b] and PTCDI-CH_3 [Hir95]. Values cited from [Pog02] are excitation energies calculated with time-dependent DFT. HOMO levels have been determined using XPS and UPS measurements.*

are difficult to control owing to the non-planar molecular structure, which results in a low degree of molecular order. Oligoacenes show the best transport properties, with a trade-off regarding the energy gap. α-Oligothiophenes exhibit good transport properties, while having singlet and triplet energies within the visible spectral range.

1.3 Outline

In Chapter 2, the physics of organic semiconductor devices, i.e. the metal-oxide-semiconductor (MOS) capacitor, the FET in unipolar and ambipolar function as well as organic light-emitting devices are introduced. Furthermore, an overview of the theoretical concepts of charge-carrier injection, transport and recombination in organic semiconductors is given. The application of inorganic semiconductor theory to organic semiconductors is briefly discussed.

Chapter 3 describes the device preparation and characterization, including gate-oxide growth and substrate cleaning, purification of organic semiconductors as well as thin-film growth by vacuum deposition. An integrated chamber for in-situ device preparation and characterization, which was designed and set up during this thesis work, is described in detail. It allows device preparation and characterization without transfer through and thus exposure to air. For device characterization, special emphasis is put on the electrical characterization, including capacitance-voltage (CV) measurements and impedance spectroscopy on metal-insulator-semiconductor (MIS) diodes, as well as on the current-voltage characteristic of organic field-effect transistors. A cryogenic probe station that was designed with and purchased from CryoVac, allows the temperature-dependent characterization of the organic thin films. Of special interest hereby is the temperature dependence of the mobility. Also, the electrical characterization of OLEDs is discussed briefly. In addition, optical characterization methods as well as X-ray diffraction (XRD) and atomic force microscopy (AFM) were used for studying the film morphology.

In Chapter 4, experimental results on *n*- and *p*-type single-layer devices are presented. This includes film growth and morphology, as well as a detailed description of charge-carrier injection and channel formation as obtained by CV measurement in *p*-type and *n*-type materials. These results are related to field-effect mobilities extracted from the characterization of field-effect devices. The transport mechanism is discussed based on temperature dependent transport measurements.

The combination of appropriate *n*-type and *p*-type materials results in an ambipolar OFET, which is described in detail in Chapter 5. Different material combinations are discussed, including pentacene and PTCDI-$C_{13}H_{27}$, *p*-4P and PTCDI-$C_{13}H_{27}$ as well as α-5T and PTCDI-$C_{13}H_{27}$. A model for the current-voltage characteristic of ambipolar